ELSEVIER

Are microcomposites realistic models of the fibre/matrix interface? I. Micromechanical modelling

P. Zinck[a], H.D. Wagner[b], L. Salmon[c], J.F. Gerard[a],*

[a]*Laboratoire des Matériaux Macromoléculaires UMR 5627 CNRS, Institut National des Sciences Appliquées de Lyon — Bât J. Verne 69621, Villeurbanne Cedex, France*
[b]*Department of Materials and Interfaces, The Weizmann Institute of Science, Rehovot 76100, Israel*
[c]*EMA, DER, Centre de Recherche EDF des Renardières, 77250 Moret-sur Loing, France*

Abstract

The ability of the microbond technique to characterise changes in the physico-chemical structure of the interface between fibre and matrix has been checked using eight epoxyde/glass fibre systems differing by their matrix chemistry, fibre surface treatments, and fibre diameter. It has been shown that the widely used average IFSS method can lead to biased results. The test is now considered as giving mode I or mixed-mode properties of the interface and not only a mode II interfacial toughness or interfacial shear strength (IFSS). Energy approaches are thus be preferred to stress criterion models. The suitability of six theoretical models was checked. Difficulties were found in determining a parameter or method effectively representative of the physico-chemical structure of the interface. The model providing the most reliable results was that of Scheer and Nairn. Significant plastic flow of the polymeric droplet was observed, leading to a questioning of the hypotheses of ideal elastic components. © 2001 Elsevier Science Ltd. All rights reserved.

Keywords: Microbond test; Interface; Epoxyde

1. Introduction

The mechanical behaviour and durability of composite materials does not depend only on the properties of each components (matrix and fibre) but also on the structure of the interface/interphase [1,2]. The effect of the interfacial layer on the properties of composite materials can be characterised by means of mechanical tests performed directly on unidirectional composites such as torsion [3], off-axis tension test [4,5], flexure [5,6] which can be combined with in situ studies [6] for obtaining information on modes of failure and interface structure. This kind of testing involves the structural parameters of the unidirectional composites and provides only trends upon the mechanical properties of the interphase. The latter can be further characterised by means of microcomposites which in turn accurately probe the effect of various parameters on the behaviour of composite materials [7]. Those model composites are composed of a single fibre embedded or partially embedded in a matrix. Two main kinds of testing can be distinguished:

- tensile tests are performed on a dogbone specimen leading to fibre fragmentation [8,9];
- the fibre is pulled out of the matrix disk or rod [10].

The latter is known as the pull-out test and has been the subject of numerous papers in the last 30 years. A serious limitation is nevertheless encountered with fine reinforcing fibres such as carbon fibres, glass fibres, and Kevlar. If the force required for pulling out is too high, the fibre will break. For fibres whose diameter ranges from 5 to 50 μm, the maximum embedded length that can be used should be in the range 50–1000 μm [11]. It is extremely difficult to keep the embedment length down to such small values and to handle such test specimens. The microbond technique has been developed to avoid such problems [11]. A small amount of matrix is deposited on the fibre in the form of a microdroplet. A microvice is used to grip the droplet and the fibre is then pulled out. This test has become of great interest in the material science community since it is relatively easy to realise in comparison with the classical pull-out test. The microbond technique has been used in many fields including aerospace, transport industry, military applications, as well as for medicinal applications. The interface between thermosets, elastomers, amorphous, semi-crystalline

* Corresponding author.

Table 1
Different fibre/matrix systems studied by the microbond technique and aim of the study

Matrix	Fibre	Parameter studied, aim	Ref.
Epoxyde	CF	Matrix fortifier	[12]
		Cure schedule	[12]
Bismaleimide	CF	Thermoplastic sizing	[13–,15]
		Matrix reinforcement	[13–15]
		Plasma treatment	[16]
Poly(phenylene sulphide) PPS	GF	Fibre surface treatment	[17]
	GF	Crystallinity	[17]
	CF	Plasma treatment	[18]
Polyurethane and latex elastomers	Polyester, aramid, HMW PE	Reaction extension before the build up of the interface	[19]
Polymethacrylate	GF	Coupling agent for dental adhesion	[20,21]
Epoxyde	UHMPE, PE, aramid	Plasma treatment	[22,23]
Epoxyde	CF	Nickel catalysed oxydation	[24]
Epoxyde	Aramid	Surface chlorosulphonation	[25]
Epoxyde, PE	GF	Surface treatment	[26]
		Fibre diameter	[26]
Polyurethane and latex elastomers	PET, LLDPE, aramid	Fibre surface treatment	[27]
		SRIM application	
Liquid crystalline copolyester PET, Nylon 66	GF		[28]
Polybutadiene terephthalate	GF		[29]
Polyethylene	CF		[30]
Epoxyde	aramid	Surface treatment	[31]
		Experimental parameters	[31]
Epoxyde	GF, CF	Experimental parameters	[11,32,33]
	Aramid		[34,35]
Epoxyde	CF, GF	Comparison with other microtests	[36–38]
Epoxyde	CF	Investigation of the mechanisms of failure	[39]

thermoplastics, liquid crystalline polymers and a great variety of fibres including glass (GF), carbon fibres (CF), and polymeric fibres (PF) (aramid, PE, PET) has been characterised. Different systems studied in the literature are presented in Table 1 together with the physico-chemical parameters studied. It can be noticed that the influence of the following physico-chemical parameters on the adhesion between fibre and matrix can be evaluated with the microbond test:

- Matrix —
  - Chemical modification.
  - Influence of fortifiers.
  - Cure schedule, crosslinking density.
- Fibre —
  - Diameter.
  - Surface treatment. GF, effect of various sizing; CF, oxidation and plasma treatment polymer sizing; PF, plasma treatment, chlorosulfonation.

Those studies can be further connected with surface spectroscopy (XPS [22,25] ESCA [40], EDX [25]) for the understanding of the improvements in adhesion mechanisms. The technique has also great potentiality in the field of durability of composites in use in a hostile environment (hot water, vapour) [40–43] and fatigue behaviour of the interface [44].

In contrast with the classical pull-out test, theoretical works devoted to the modelling of the test is relatively rare and difficult to apply to experimental results. Thus, the average interfacial shear strength (IFSS) is generally used to characterise the influence of the studied parameter. This approach implies a constant shear stress along the interface [45] which is in fact not the case as shown by finite element analysis (FEA) [46,47] and Raman experiments [48]. Another way consists of using some of the numerous models developed for the classical pull-out test even if the experimental configuration differs. This was done in previous work [17] and leads to irregularities such as values of interfacial parameters without physical meaning. Based on SEM photographs showing plastic flow of the polymeric droplet, the applicability of those models which consider ideal elastic components is also in doubt [17].

Another limiting aspect is the important data scatter usually observed for micromechanical testing. A round-robin program [36] conducted for this purpose a few years ago suggested the need to establish standard procedures for reducing the inter-laboratory scatter. It was also shown that

Table 2
Mechanical and thermal properties of the considered E-glass

Fibre	Diameter (μm)	Standard deviation (μm)	Weight loss[a] (wt%)	Sizing thickness[b] (nm)	Average tensile stress (GPa); gauge length 20 mm
Water-based sizing (WS)	18.1	1.4	–	–	1.92
A1100 treated	18.3	1.7	0.17	21	2.02
P122 1200 Tex	19.1	1.4	0.77	86	1.75
P122 2400 Tex	26.6	2.0	0.55	86	1.42

Tensile modulus (GPa)		Poisson's coefficient		Thermal expansion factor (K^{-1})	
73		0.22		5×10^{-6}	

[a] Determined from TGA analysis.
[b] Calculated assuming a continuous sizing layer.

intra-laboratory scatter cannot be attributed to operator change [16] and thus seems to be inherent to this kind of testing involving many experimental parameters. Studies dealing with the influence of these experimental parameters were also conducted [32,35,39] and it can be concluded that, for obtaining satisfactory and reliable results, the experimental configuration must be, if not perfectly controlled, at least kept constant.

The aim of this paper is to show that the microbond technique is a very powerful tool for characterising adhesion at the interface, but it has to be used *carefully*. The suitability of theoretical models will be assessed on glass fibre/ epoxyde systems differing by their chemistry, surface treatment and diameter. Based on these experiments, the difficulty in defining a parameter which is effectively representative of the physico-chemical structure of the interface will be emphasised.

2. Experimental section and results

2.1. Materials

E-glass fibres have been supplied by VETROTEX Int. Three different types of fibres differing by their surface treatments have been considered:

- A "water-based sizing" (WS) treatment corresponding to the deposition of an aqueous solution of an antistatic agent.
- A silane-based treatment corresponding to the deposition of γ-aminopropyltriethoxysilane (denoted A1100) from a 1 wt % aqueous solution of silane.
- Commercial sizing referred to as P122 by Vetrotex Co., known as a "universal sizing", i.e suitable for epoxyde as well as polyester matrices. The coupling agent included
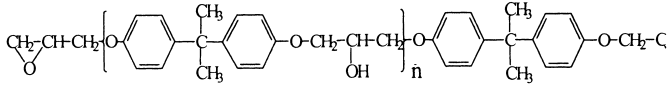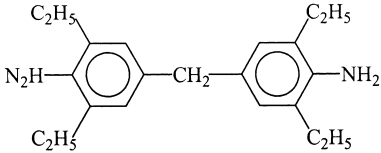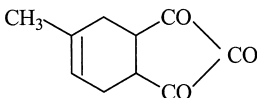
Table 3
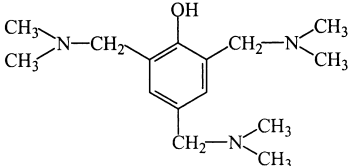Comonomers used in the epoxyde formulations

Name	Formula	Av. molar mass (g/mol)	Supplier
DGEBA $n = 0.15$		381.2	Ciba Geigy
MDEA		310.5	Lonza
MTHPA		166	Anchor Chemical
DMP30		263	Fluka

Table 4
Cure schedule of the epoxyde networks

Matrix	Cure (h, °C/min)	Post-cure (h, °C/min)	Heating rate (°C/min)	Cooling rate (°C/min)
DGEBA/MDEA	4, 135	4, 190	2	1
DGEBA/MTHPA	1, 100	5, 160	2	1

in this sizing formulation was the A1100 (concentration of 1 wt%). Other constituents such as a lubricant and a film former were also included. Two different P122 references, namely 1200 Tex and 2400 Tex, with different fibre diameter have been considered.

The fibre diameter was measured by optical microscopy with a sample size of 100. Results are given in Table 2 together with mechanical properties. The amount of sizing (by weight) was determined by thermogravimetric analysis under an inert atmosphere (heating rate: 5 K/min) and the thickness of the deposit layer was estimated assuming a continuous layer. Matrices considered in this study are polyepoxies based on diglycidyl ether of bisphenol A (DGEBA). Two different hardeners were selected, 4,4′- methylene-bis[2,6-diethyleneaniline (MDEA) and anhydride *cis*-4-methyl 1,2,3,6-tetrahydrophtallic (MTHPA) leading to two different chemistries i.e polycondensation between amine and epoxyde functions and chain polymerisation between epoxyde and anhydride functions. The latter requires the use of an accelerator. A tertiary amine was selected for this purpose, 2,4,6-(dimethyl aminomethylene) phenol (DMP30). All reactions were conducted for radii epoxyde/anhydride = 1 and epoxyde/amine = 1. The amount of accelerator for the epoxyde/anhydride reaction was set to 1.5 wt%. Chemical formulae, average molar weight and suppliers are presented in Table 3. The chosen radii and the cure schedule (Table 4) lead to a fully cross-linked network as revealed by DSC thermograms. The glass transition temperature was measured by differential scanning calorimetry. Young's modulus and Poisson's ratio used for modelling the experimental data were determined in tension using a Adamel Lhomarghy DY22 apparatus at a cross-speed of 0.5 mm/min. The thermal expansion coefficient was determined on a DMA 2980 (TA Instrument) using a penetration clamp at 2°C/min. The yield point was measured in compression using the same apparatus. The physical and mechanical properties of the cured networks are presented in Table 5.

2.2. Microbond specimens

Microbond specimens were prepared by first mounting horizontally the glass fibres on a frame with a prestrain of 300 MPa for the WS, A1100 and P122 1200 Tex and 160 MPa for P122 2400 Tex to avoid random manual prestraining which can weaken the fibre and lead to an underestimation of the interface properties. WS fibres were first washed with THF and hexane for 15 min, respectively. Prepolymers and hardeners were mixed at room temperature for the MTHPA system and at 60°C for DGEBA/MDEA since the amine is in solid form at room temperature (melting point 88°C). A single filament was used to form droplets on the fibre. The microdroplets were allowed to react at room temperature for 48 h in order to avoid vapourisation of the hardener [37]. The cure schedule is that specified in Table 4. A typical specimen is presented in Fig. 1.

2.3. Adhesion measurements

Symmetrical droplets were selected. The droplet/fibre specimen was stuck at one end to a piece of PET and suspended on the cross-head of a tensile tester equipped with a 5 N load cell. A rigid epoxyde adhesive was used to ensure that no deformation at the PET/fibre interface could occur during the experiment. Special care was taken to obtain samples with a free length as short as possible. Tests were performed at a cross-head speed of 0.5 mm/min. The microbond shearing device and a typical force/extension graph are presented in Figs. 2 and 3, respectively. Tests were conducted until 35–40 debonded specimens were obtained. Figs. 4 and 5 show the maximum debonding load with respect to the embedded length for the different systems tested. The important experimental scatter observed is inherent to this kind of testing, as discussed in Section 1. In order to assess the influence of the various physicochemical parameters, it is necessary to use one of the numerous theoretical analyses devoted to microcomposites.
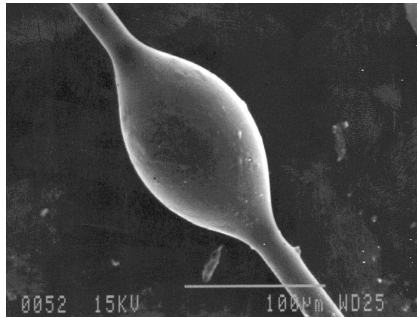
Table 5
Mechanical and physical properties of the epoxy networks

Matrix	T_g (°C)	E (GPa)	ν	Yield point (MPa)	$\alpha.(\times 10^4 \, \mathrm{K}^{-1})$
DGEBA/MDEA	158	3.35	0.41	105.5	1.18
DGEBA/MTHPA	124	3.89	0.37	108.4	0.75

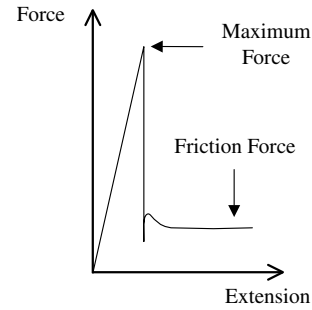Fig. 1. Typical microbond specimen — system DGEBA/MDEA/A1100.

Fig. 3. Typical force versus extension recording.

3. Modelling interfacial adhesion data

3.1. General comments

We will begin this part by brief considerations upon the three possible failures modes of the interface as proposed by Piggott [49]:

1. Failure occurs when the maximum shear stress reaches the interface shear strength. The shear stress at the interface, which has a maximum value at the gripped end of the droplet can then be derived from the shear-lag assumption [50,51]. This analysis considers tensile stresses in the matrix and shear stresses in the fibre negligible in comparison with shear stresses in the matrix and tensile stresses in the fibre, respectively:

$$\tau_f \ll \sigma_m$$

$$\tau_m \ll \sigma_f$$

2. The interface yields if its yield stress is reached. A constant shear stress distribution can be assumed along the interface and a simple force equilibrium gives the value of the interfacial yield stress [45]. Due to its simplicity, this is the most widely spread approach and known as the average IFSS method.
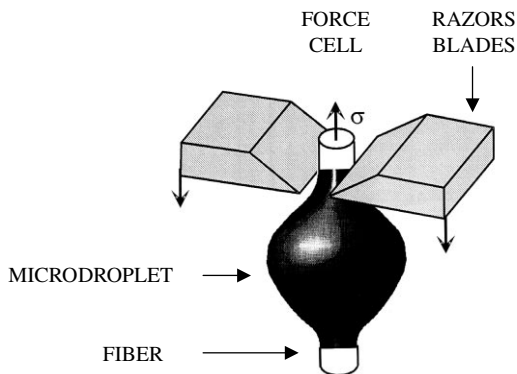3. The interface fractures with a work of fracture G_{ic}.

Fig. 2. Microbond shearing device.

Initiation occurs at the maximum stress point (approximately where the fibre emerges from the matrix) and the fracture propagates rapidly along the interface.

According to those considerations, the approaches considered in the literature can be divided in two categories, i.e. the fracture is described in terms of a critical stress or by the use of an energetic parameter. Among those numerous theoretical analyses only one recently proposed is devoted to the specific microbond configuration [52]. Thus, authors considered the calculation of the average IFSS or the use of the models initially developed for the classical pull-out configuration [17].

In this context, we reconsidered some 15 theoretical approaches and compared them, by considering the different hypothesis and phenomenon taken into account in the modelling. This is summarised in Tables 6 and 7 for stress criterion and energy criterion models, respectively. It should be noted there that a distinction is made concerning the description of the failure in terms of crack initiation followed by a catastrophic failure, or a steady-state crack propagation. A stability criterion is proposed in some models. Consider also the different hypothesis taken into account in each model, and in particular the residual stresses, which are only dealt with in two analyses [52,55–57]. How can we choose, in this context, among those numerous theoretical approaches, the most pertinent one ?

3.2. Models selection

The calculation of the average IFSS, that we will referred to as IFSS method is of great interest, due to its simplicity of use. It is nevertheless essential to compare the results obtained with more complete approaches, since many parameters are changing from one system to another, the mechanical and physical properties of the polyepoxyde networks for instance. It seems also of great interest to compare the stress criterion and the energy models, and finally to confront the result with the model developed specifically for the microbond configuration. In fact, the problematic is to know whether or not it is necessary to use a heavy formalism to treat the data, or if the simplistic IFSS method is enough, especially for a study devoted on
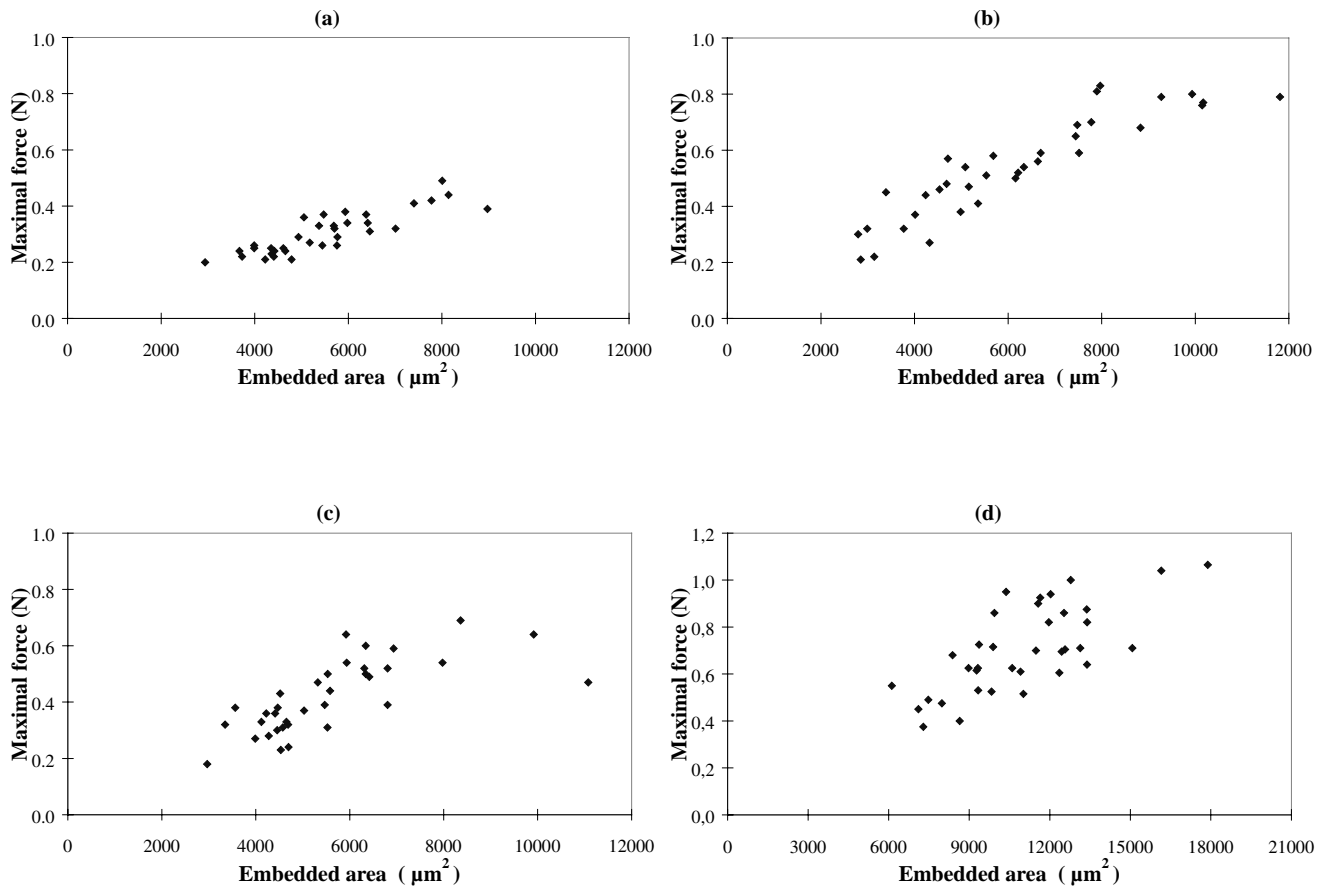
Fig. 4. Debonding load with respect to embedded length for the epoxyde/amine network with: (a) WS fibre, (b) A1100, (c) P122 1200 Tex, (d) P122 2400 Tex.

the influence of the physico-chemical nature of the components on the interfacial adhesion. In the light of those considerations, and for reasons that will be highlighted later, we choose to fit the experimental data according the following theoretical analyses:

- IFSS and the model of Greszczuk [50] for the stress criterion models.
- Piggott [49] and Penn and Lee's [65] models for the energy based approaches.
- Two micromechanical treatments proposed by Scheer and Nairn [52] for the specific microbond configuration.

3.3. Quantitative results

The formalism of the different approaches is briefly presented in Appendix A. Greszczuk, Piggott and Penn and Lee models are based on two adjustable parameters:

- a length up to which the shear stress in the matrix reach the value 0, generally abusively considered as representative of the interphase thickness $(b - R)$;
- the maximum interfacial shear stress τ in the microcom-

posite in the vicinity of the microvice, or the interfacial toughness G_{ic}.

The models proposed by Nairn consider only G_{ic}. Data have been fitted according to two approaches, derived from the shear-lag theory and the variational mechanics, respectively. As proposed by the authors, the latter was considered in a simplified form, valuable for microdroplets exhibiting a length/diameter ratio greater than 5, which was full-filled for the systems considered in this study. The pre-crack conceptualised in Penn's model is considered negligible in comparison with the embedded length. A classical least-squares method enabled to fit the experimental data from Figs. 4 and 5. The results are presented in Table 8. It can be seen that the trends concerning the influence of the physico-chemical nature of the components on the interfacial adhesion, as given by the values of the different interfacial parameters are in very poor agreement. Stress criterion approaches, i.e. average IFSS and Greszczuk's model provide nevertheless similar trends. Note important discrepancies, such as values of the interphase thickness (b in Greszczuk's model) greater than the actual droplet diameter. The same parameter is more realistic when obtained by energetic approaches (R). However, the influence of the nature of the components is still unclear
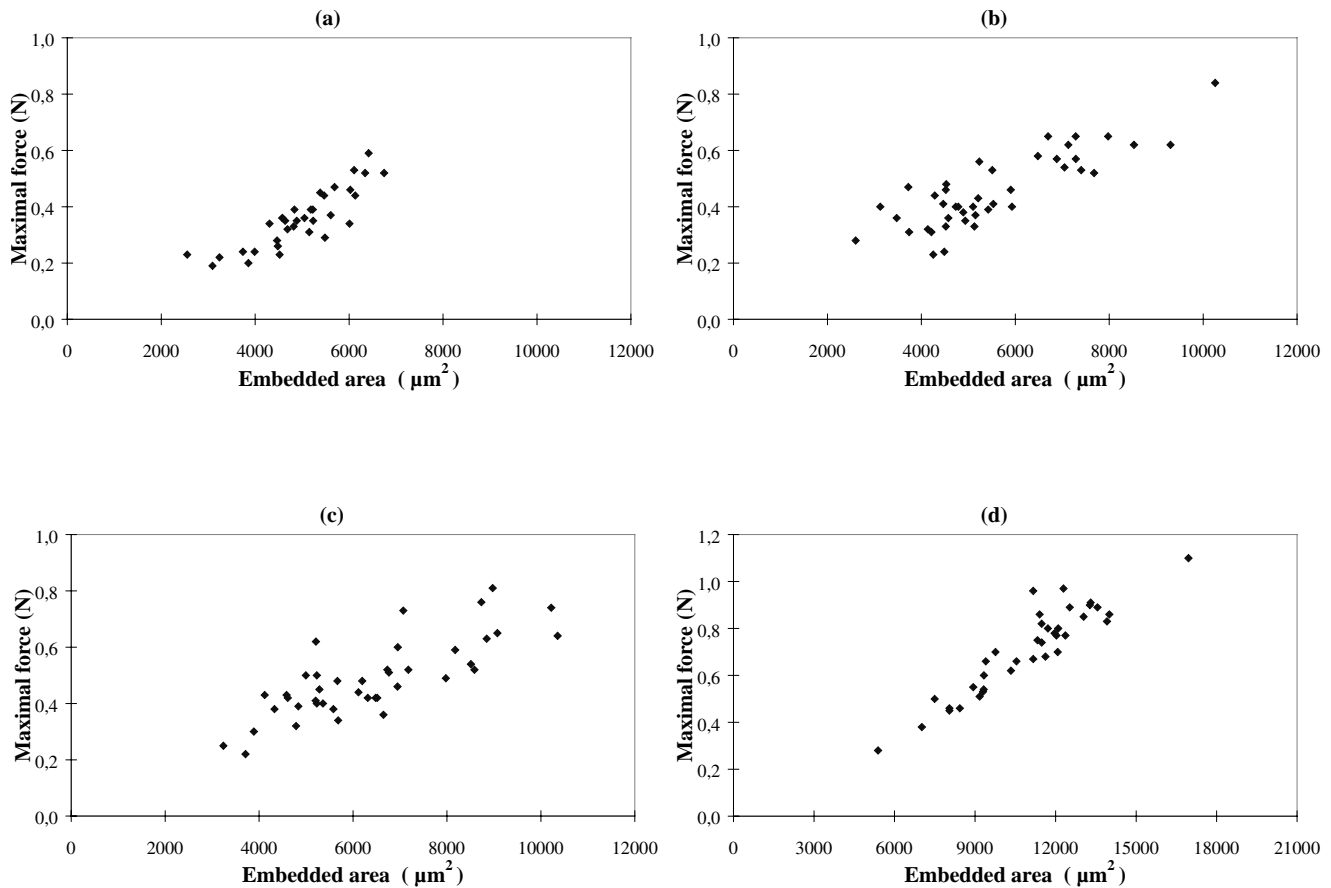
(a)

(b)

(c)

(d)

Fig. 5. Debonding load with respect to embedded length for the epoxyde anhydride network with: (a) WS fibre, (b) A1100, (c) P122 1200 Tex, (d) P122 2400 Tex.

when considering those models, in particular for the epoxyde/anhydride system. A critical analysis of those theoretical analyses is thus necessary before extracting the exact influence of the physico-chemistry on the interfacial adhesion.

4. Critical analysis of the models

4.1. Stress distribution at the interface and modes of failure

Works devoted to the distribution of stresses in the vicinity of the interface during testing were experimental (involving Raman spectroscopy [48], photoelasticimetry [68]) as well as numerical (FEA [46,47,69]). They concluded that the IFSS is not constant along the interface, but shows a maximum at a distance from the gripped end of the droplet ranging from 1/10 to 1 fibre diameter. Several parameters do influence the height of this peak, including:

- Young modulus of the matrix [69].
- Fibre diameter [69].
- Embedded length [69].
- Residual shrinking stresses [48].

- Interphase modulus [46].
- Loading configuration [68].

Radial stresses at the interface were also characterised using FEA analysis [68]. They are tensile at the point where the fibre emerges from the droplet, decrease rapidly to zero and then become compressive. It is now well accepted that they play an important role in the failure initiation. One important consequence of these radial stresses on the pull-out experiment is that initiation of debonding is now considered as pure mode I fracture in the case of the microdroplet [52] and a mixed-mode failure with predominating mode I in the classical pull-out configuration [70]. This mechanical consideration is confirmed by post-mortem observations of the failure location, showing a residual meniscus of polymer (Fig. 6). This consistent with a cohesive fracture of the polymeric droplet, showing evidence of mode I feature. One should argue at this step of the progression that, under these considerations, and if debonding is controlled by the initiation of the interfacial crack, the test should be representative of the mode I or mixed-mode feature of the matrix, in other words, the toughness of the network. This is fortunately not the case. Hodzik et al. [71] have shown by FEA that the contact angle between the fibre and the

Table 6
Stress criterion models — σ_m and σ_f are the tensile stress in the matrix and the fibre, respectively, and τ_m the shear stress in the matrix

Author	Year	σ_m	σ_f	τ_m	Friction	Poisson effect	Residual stresses
Greszczuk [50][a]	1969	0	1	1	0	0	0
Lawrence [53]	1972	0	1	1	1	0	0
Takaku and Arridge [54]	1973	0	1	1	1	1	0
Hsueh [55–57]	1989	1	1	1	1	1	1
Yue and Cheung [58,59]	1992	1	1	1	1	1[b]	0

[a] The only model considering a catastrophic failure of the interface is that of Greszczuk.
[b] A different approach is considered in order to take into account the Poisson effect in the fibre.

epoxyde prepolymer mixture, and in turn, the surface treatment applied to the fibre, plays a preponderant role in the failure mechanism. It must then be emphasised that, if debonding is controlled by the initiation of the interfacial crack, the microbond test should be considered as measuring the mode I or mixed-mode failure properties of the interface and not an IFSS or mode II interface toughness. Considerations upon phenomenological aspects of the failure are now required in order to answer this question.

4.2. Phenomenological aspects and average IFSS method

In this part, interpretation of the load versus extension rate trace for the classical pull-out test reported by DiFrancia et al. [72] are presented. The theoretical embedded fibre length with respect to the maximum load curve presented in Fig. 7 can be divided into three parts:

(i) The initiation of the failure is immediately followed by catastrophic interfacial failure and the load increases with increasing embedded length.
(ii) Complete debonding does not occur as a catastrophic failure because of the friction along the debonded length. Energy is dissipated via this friction and the load increases with increasing embedded length.
(iii) A steady state propagation is observed. The fibre contracts due to Poisson effect and friction forces become

negligible. The maximum load is constant with respect to the embedded length.

This imply that for cases (ii) and (iii), the debond initiates well before reaching the maximum force. This has been confirmed experimentally by Marotzke et al. [70] on a glass fibre/polystyrene system for the classical pull-out configuration. It was further reported that "the evaluation of the maximum force in order to determine an IFSS is not reasonable since this is not representative of the IFSS". This is in agreement with the non-linearity of the debond strength versus embedded length trace usually observed. Those considerations together with the variation of the shear stress distribution along the interface allow us to claim that *the average IFSS method which is widely used in the literature is probably incorrect*. It is thus of great importance to compare this simple method with more complete models in order to check the reliability of the results provided by this method. The second important implication of those considerations is that the nature of the information delivered by the test is strongly influenced by the value of the embedded length L_e.

4.3. Implications concerning the exploitation of experimental data

For small embedded lengths, it is assumed that initiation

Table 7
Energetic criterion models — σ_m and σ_f are the tensile stress in the matrix and the fibre, respectively, and τ_m the shear stress in the matrix

Authors	Year	Energy — fibre σ_f [a]		Energy — matrix			Other parameters		
		Free	Embedded	σ_m	τ_m	Friction	Residua stresses	Poisson effect	Pre-crack
Outwater and murphy [60]	1969	0	1	0	0	1	0	0	0
Bowling and Groves [61]	1979	0	1	0	1	1	0	1	0
Wells and Beaumont [62]	1985	0	1	0	0	1	0	1	0
Stang and Shah [63]	1986	0	1	0	0	0	0	0	0
Piggott [49]	1987	0	1	0	1	0	0	0	0
Gao et al. [64]	1988	0	1	1	0	1	0	1	1
Penn et al. [65]	1989	1	1	0	1	0	0	0	1
Mai et al. [66,67]	1992	0	1	1	1	1	0	1	1
Scheer and Nairn [52]	1995	0	1	1	1	0	1	0	1

[a] The fibre shear strain is only considered in Scheer and Nairn's model.

Table 8
Tabulated parameters from the fitting of the data according to six approaches

Matrix	Fibre	Average IFSS (MPa)	Standard deviation (MPa)	τ_{max} Greszczuk (MPa)	b (μm)	G_{ic} Piggott (J/m^2)	R (μm)	G_{ic} Penn and Lee (J/m^2)	R (μm)	G_{ic}–Scheer shear-lag (J/m^2)	G_{ic}–Scheer variational (J/m^2)
MDEA	WS	56	7 (12%)	56	> 200	364	2.09	386	2.18	95	99
MDEA	A1100	89	14 (16%)	100	> 200	885	1.01	971	1.03	239	243
MDEA	P122 12	80	20 (25%)	75	> 200	576	0.12	687	1.11	185	189
MDEA	P122 24	65	12 (18%)	64	> 200	471	2.51	517	2.78	185	192
MTHPA	WS	71	11 (15%)	73	100	713	2.09	739	2.15	201	201
MTHPA	A1100	84	17 (20%)	83	> 200	854	2.12	918	2.23	250	251
MTHPA	P122 12	77	14 (18%)	82	> 200	667	2.28	715	2.3	246	246
MTHPA	P122 24	65	7 (11%)	67	> 200	604	1.01	646	1.02	270	270

of the failure leads to complete debonding. The maximum load is then representative of initiation, and thus, according to previous considerations, representative of mode I or mixed-mode failure properties of the interface.

For greater embedded lengths, the maximum load includes two components, initiation in mode I or mixed-mode and propagation of the crack in mode II. Careful observations during the test have shown that the criterion of steady state crack propagation actually depends on the embedded length, and that for great L_e, the initiation occurs well before the strength reaches its maximum. From a more formalistic point of view:

- For small embedded lengths (case (i)), $F_{MAX} = F_{init}$.
- For cases (ii) and (iii), F_{MAX} is representative of both initiation and propagation of the crack, and thus, a mode I or mixed-mode and II characteristic.

Let us now consider L_{cata}, the embedded length for which the slope changes on the maximal force versus embedded length. Exploitation should be performed as follows:

- For $L_e < L_{cata}$, $F_d = F_{MAX} = F_{init}$.

- For $L_e > L_{cata}$, F_{init} is the point where the slope changes and $F_d = F_{MAX}$.

where F_{MAX} is the maximum force on the load extension graph, F_{init} the load at which the failure is initiated and F_d the debonding force. A rigorous treatment of the experimental data should thus be performed by making a distinction between both cases, and by considering models describing initiation followed by catastrophic crack propagation and steady state propagation, respectively. It is thus necessary to determine L_{cata}, the embedded length for which the propagation becomes catastrophic. Different methods can be considered:

- Marotzke and Hampe [70] observe a slope change in the strength — length curve corresponding to the crack initiation. This was not the case for our systems.
- Difrancia et al. [72] propose to determine L_{cata} from the F_d–L_e curve (Fig. 7). This is not possible here, due to the important scatter usually observed (see Figs. 4 and 5).
- One can also note during the test at which force initiation occurs. This was unfortunately not realised for our experiments.
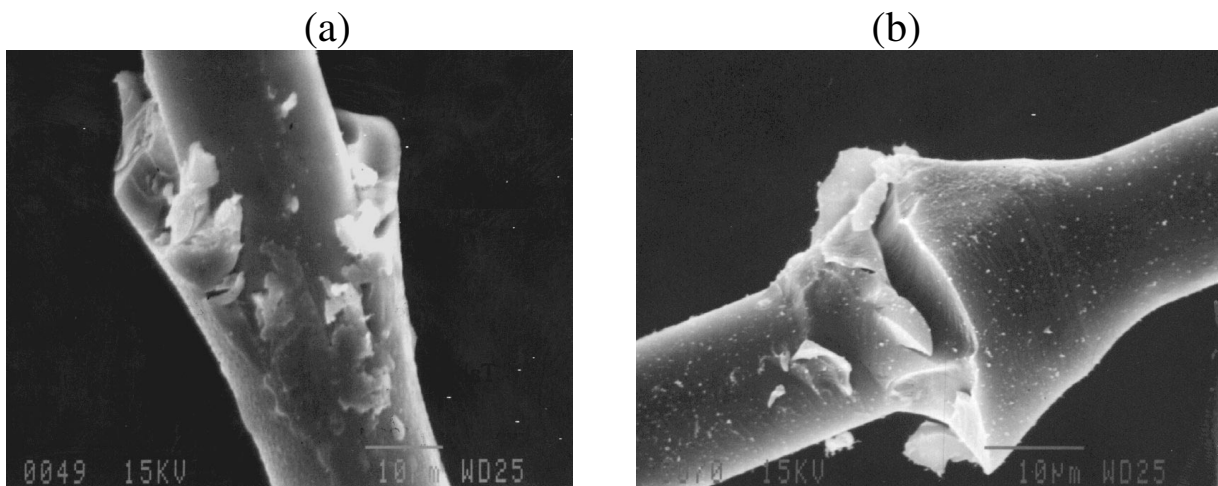
(a)   (b)

Fig. 6. SEM observations of the meniscus for two systems: (a) epoxyde/amine/A1100, and (b) epoxyde/anhydride/P122 1200 Tex.
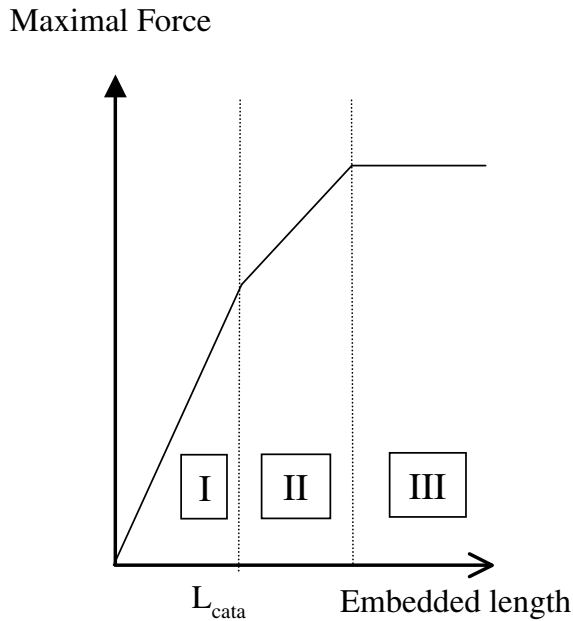
Maximal Force

Fig. 7. Theoretical load versus embedded length curve after Ref. [72].

Considering the small-embedded lengths tested, the ratio of microcomposites exhibiting a steady state propagation of the crack remained altogether weak. We thus choose to use models describing fracture initiation. The microbond test applied to our systems is thus considered as describing the mixed-mode properties of interfaces.

4.4. Intermediary considerations

At this step of our progression, we have shown that:

- The average IFSS method, which is widely used in the literature, does not represent a satisfactory interfacial parameter
- Different kinds of information are delivered by the microbond test, according to the embedded length, and can lead to difficulty concerning the modelling. For our systems which present a strong interface, the crack mostly propagates in a catastrophic way.
- The failure is thus governed by crack initiation, which occurs in mixed-mode and not mode II. It is thus more convenient to use energy criterion models instead of maximum shear stress approaches. We join the conclusions of Zhandarov et al. [73], who showed that the critical shear strength obtained by the microbond test is diameter dependent, a geometrical parameter which is in fact not representative of the physico-chemical properties of the interphase, whereas G_{ic} is absolutely geometry-independent. For these authors, interface failure is clearly governed by an energy criterion.

We have at this step eliminated two of the five selected approaches. We have now to confront energy criterion
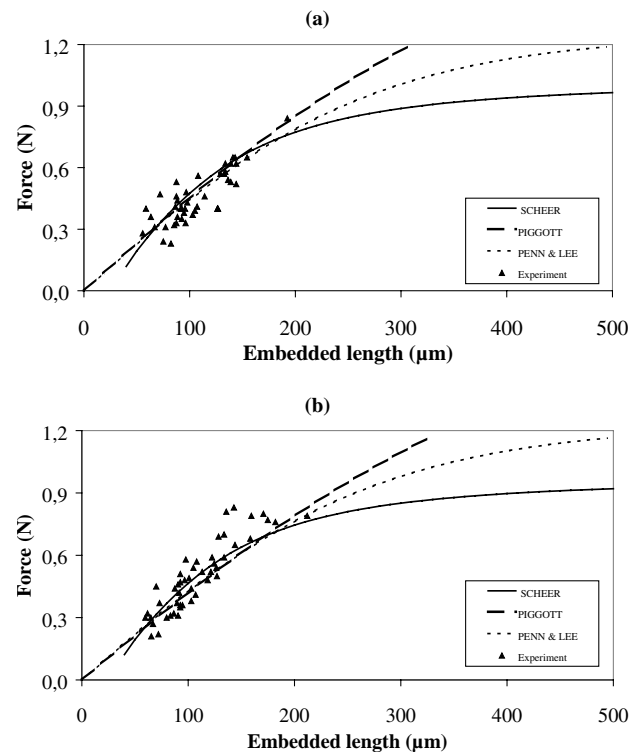

Fig. 8. Confrontation of energy models with experimental data for: (a) epoxyde/amine/A1100, and (b) epoxyde/anhydride/A1100 microcomposites.

models in order to extract the physico-chemical contribution of the components.

4.5. Critical comparison of energy models — on the importance of residual stresses

The quality of the fitting of the experimental data by energetic approaches can be graphically appreciated in Fig. 8. Due to the important experimental scatter, it is very difficult to distinguish differences between the models. It should be noted there that the data have been obtained for small values of the embedded length. The smallest asymptotic value is obtained with the approach of Scheer and Nairn. These authors highlighted some limits of the energy criterion models:

- A total energy criterion is considered in the formalism of Piggott — the energy per unit length equals the interface toughness, and this is in no way a linear elastic fracture mechanic criterion.
- Penn and Lee used a correct energetic criterion by considering a pre-crack, but the influence of the external work on G_{ic} is not taken into account in the modelling.

Both approaches exhibit thus an incomplete energy balance. In addition to those formalistic considerations, it must be noticed that the model specific to the microbond configuration is for the moment the most complete one: tensile
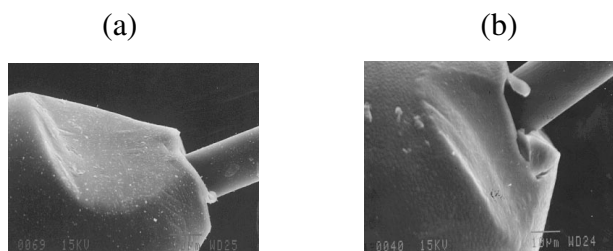
(a) (b)

Fig. 9. Plastic flow of the polymeric droplet — systems (a) epoxyde/anhydride/P122 1200 Tex, and (b) epoxyde/amine/A1100.

Fig. 10. Fracture energy of interphases for the anhydride (black) and amine (grey) hardened polyepoxyde/glass fibre microcomposites.

stresses in the matrix and shear stresses in the fibre are considered, as well as residual stresses. We should address a special issue on this topic which is generally neglected and poorly known. Residual stresses have a great influence on what we will refer to as the mechanical part of interfacial adhesion, as opposed to the physico-chemical contribution. Among other parameters, they are strongly dependent on the glass transition temperature of the epoxyde network, and their level is considerably higher for the DGEBA/MDEA system [74]. It is thus of great importance to take residual stresses into account in the treatment of experimental data.

4.6. Limit of theoretical approaches: the hypothesis of ideal elasticity

An important plastic flow of the polymeric microdroplet can be observed on the samples after the test (Fig. 9). It must be kept in mind that all the models considered in this study assume a linear elastic behaviour of the component, which is actually not true. This leads to an over-estimation of the interface toughness, since a part of the energy is lost via this dissipative process. This phenomenon may not be specific to our thermosetting systems, since it has been reported in the literature for thermoplastic matrices [17]. Theoretical analysis could be reviewed in order to include this energy dissipation via plastic flow. This should be possible via the J integral, which is a better criterion for dissipative systems than G [75].

5. Influence of the nature of the components

Finally, we should address our first issue, the influence of the physico-chemical nature of the components on the interfacial adhesion. It seems difficult to select a parameter or a method which is effectively representative of the physico-chemical structure and properties of the interface. All models are not able to detect changes in interfacial adhesion, and this can lead to biased trends. The use of a relatively heavy formalism is thus justified for the microbond technique. Fracture energies of the interphases of the different systems according to Nairn's approach are presented in Fig. 10. The values are in agreement with 223 J/m^2 reported for a polyepoxyde/glass fibre system [52]. The methodology
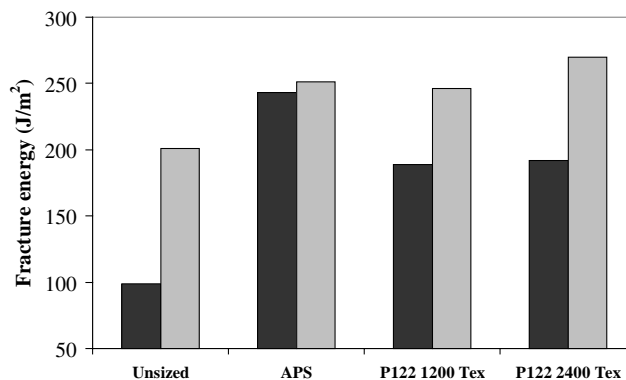
enables to detect changes in adhesion according to:

- A matrix modification — the epoxyde/anhydride system leads to interface properties slightly stronger than the epoxyde/amine network. It should be noticed there that opposite trends are given by the stress approaches. This could be attributed to the residual shrinking stresses.
- The differences between different sizing and surface treatments. In this case, the same trends are observed for each models. The strongest interface is obtained when using a coupling agent alone, whereas a weak interface results from the absence of surface treatment.
- The influence of the diameter is much more delicate to detect. Moon et al. [26] have shown that an increase of the fibre diameter leads to a decrease of the IFSS, which is actually the case in this work. This parameter is nevertheless not representative of the nature of interfacial zones, and the energy approaches show an altogether diameter independent interfacial toughness.

6. Conclusions

This work devoted to the ability of the microbond technique to characterise adhesion between fibre and matrix has shown that this technique is a powerful tool. The microbond test is now considered as giving mode I or mixed-mode interface properties, and not a mode II interfacial toughness or an IFSS. Energy based approaches should thus be preferred instead of maximum stress criterion. In particular, the use of the average IFSS as a parameter representative of the physico-chemical structure of the interface should be avoided. Even if it can characterise the improvement brought by a surface treatment, biased results can be obtained when comparing different matrices. This can be due in part to residual shrinking stresses and thus more complete models have to be used, such as that of Scheer and Nairn which account for internal stresses. Plastic flow of the polymeric droplet has been observed, leading to

questioning about the hypotheses of ideal elastic components.

Acknowledgements

Appendix A. Theoretical analyses

Greszczuk analysis

$$\tau_{max} = \frac{F_{max}}{2\pi r_f} \alpha \coth(\alpha L_e)$$

$$\alpha = \sqrt{\frac{2G_{int}}{br_f E_f}}$$

Piggott analysis

$$F_{max} = 2\pi r_f \sqrt{E_f G_{ic} L_e n \tanh\left(\frac{nL_e}{r_f}\right)}$$

$$n = \sqrt{\frac{E_m}{E_f(1 + \nu_m) \ln\left(\frac{R}{r_f}\right)}}$$

Penn and Lee analysis

$$F_{max} = \frac{2\pi r_f \sqrt{r_f G_{ic} E_f}}{\sqrt{1 + \operatorname{csch}^2\left(\frac{nL_e}{r_f}\right)}}$$

Scheer and Nairn analysis

The simplified analysis derived from variational mechanics leads to

$$\sigma_d(\rho) = -\frac{D_{3s}\Delta T}{C_{33s}} + \sqrt{\frac{2G_{ic}}{r_f C_{33s}} + \frac{\Delta T^2}{C_{33s}}\left(\frac{D_{3s}^2}{C_{33s}} - \frac{D_3^2}{C_{33}}\right)}$$

The shear-lag analysis provides

$$\sigma_d(\rho) = -\frac{D_{3s}\Delta T}{C_{33s}} + \sqrt{\frac{2G_{ic}}{r_f C_{33s}}}$$

where σ_d is the stress at decohesion and ρ the axial ratio (embedded length/fibre diameter), the C and D constants depends on the sample dimensions and on the mechanical properties of the fibre and the matrix:

$$C_{33s} = \frac{1}{2}\left(\frac{1}{E_F} + \frac{V_f}{V_m E_m}\right)$$

$$D_{3s} = \frac{1}{2}(\alpha_f - \alpha_m)$$

$$C_{33} = \frac{1}{2}\left(\frac{1}{E_F} + \frac{V_f}{V_m E_m}\right) - \frac{V_m A_3^2}{V_f A_0}$$

$$D_3 = -\frac{V_m A_3}{V_f A_0}[\alpha_T - \alpha_m] + \frac{1}{2}(\alpha_f - \alpha_m)$$

$$A_0 = \frac{V_m(1 - \nu_T)}{V_f E_T} + \frac{1 - \nu_m}{E_m} + \frac{1 + \nu_m}{V_f E_m}$$

$$A_3 = -\left(\frac{\nu_f}{E_f} + \frac{V_f \nu_m}{V_m E_m}\right)$$

In these equations, r_f is the fibre radius, L_e the embedded length, G_{int} the interphase shear modulus, G_{ic} the critical energy release rate, R an axial distance up to which the shear stress is zero in the matrix, b the width of the matrix under shear stress, E_f and E_T the axial and transverse tensile moduli of the fibre, ν_f and ν_T the axial and transverse Poisson's ratio of the fibre, α_f and α_T the axial and transverse thermal expansion coefficients of the fibre, E_m, ν_m and α_m the tensile modulus, Poisson's ratio and thermal expansion coefficient of the matrix. V_f and V_m are the volume fraction of the fibre and the matrix, respectively. According to the work of Scheer and Nairn for theoretical predictions, they were calculated from the plot measured droplet diameter versus measured droplet length curve.

References

[1] Drzal L. Adv Polym Sci 1985;75:1.
[2] Gérard JF, Chabert B. Macromol Symp 1996;108:137.
[3] Lacrampe V. PhD thesis, Institut National des Sciences Appliquées, France, 1992.
[4] Nemeth MP, Herakovich CT, Post D. Compos Technol Rev 1983;5:61.
[5] Zinck P, Lacrampe V, Gérard JF. Rev Compos Mater Av 1997;7:31.
[6] Gérard JF. Polym Engng Sci 1988;28:568.
[7] Wagner HD, Rubins G, Marom G. Polym Compos 1991;12(4):233.
[8] Kelly A, Tyson WR. J Mech Phys Solids 1965;13:329.
[9] Kelly A, Tyson WR. J Mech Phys Solids 1966;14:177.
[10] Mooney RD, McGarry FJ. Proceedings of the 14th Annual Technical Conference on Reinforced Plastics Division. Society of the Plastic Industry, 12-E, 1959.
[11] Miller B, Muri P, Rebenfeld L. Compos Sci Technol 1987;28:17.
[12] Biro DA, McLean P, Deslandes Y. Polym Engng Sci 1991;37(17):1250.
[13] Liao YT, Lin CH, Liu WL. Appl Polym Sci Notes 1990;40:2239.
[14] Liao YT, Lee KC, Lin CH, Liu WL. 35th International SAMPE Symposium, 1990.
[15] Liao YT, Lee KC. J Appl Polym Sci Notes 1992;44:933.
[16] Heisey CL, Wood PA, McGrath JE, Wightman JP. J Adhes 1995;53:117.
[17] Gonon L, Momtaz A, Van Hoyweghen D, Chabert B, Gérard JF, Gaertner R. Polym Compos 1996;17:265.
[18] Yuan LY, Shyu SS, Lai JY. J Appl Polym Sci 1991;42:2525.
[19] Epstein M, Shishoo RL. J Appl Polym Sci 1993;50:863.

[20] McDonough WG, Antonucci JM, Dunkers JP. Polym Preprints 1997;38(2):112.

[21] McDonough WG, Antonucci JM, Dunkers JP. Proceedings of the 21st Annual Meeting of the Adhesion Society, 129, 1998.

[22] Biro DA, Pleizier G, Deslandes Y. J Mater Sci Lett 1992;11:698.

[23] Biro DA, Pleizier G, Deslandes Y. J Appl Polym Sci 1993;47:883.

[24] Rearick BK, Harisson IR. Polym Compos 1995;16(2):180.

[25] Sheu GS, Lin TK, Shyu SS, Lai JY. J Adhes Sci Technol 1994;8(5):511.

[26] Moon CK, Lee JO, Cho HH, Kim KS. J Appl Polym Sci 1992;45:443.

[27] Epstein M, Shishoo RL. J Appl Polym Sci 1995;57:751.

[28] Sauer BB, DiPaolo NV. J Adhes 1995;53:245.

[29] McAlea KP, Besio GJ. Polym Compos 1988;9(4):285.

[30] Moon CK, Cho HH, Lee JO, Park TW. J Appl Polym Sci Notes 1992;44:561.

[31] Wagner HD, Gallis HE, Wiesel E. J Mater Sci 1993;28:2238.

[32] Gaur U, Miller B. Compos Sci Technol 1989;34:35.

[33] Miller B, Gaur U, Hirt DE. Compos Sci Technol 1991;42:207.

[34] Chou CT, Gaur U, Miller B. Compos Sci Technol 1994;51:111.

[35] Chou CT, Gaur U, Miller B. J Adhes 1995;53:33.

[36] Pitkethly MJ, et al. Compos Sci Technol 1993;48:205.

[37] Rao V, Herrera-Franco P, Ozzello AD, Drzal LT. J Adhes 1991;34:65.

[38] Yavin B, Wagner HD. Adv Compos Lett 1993;2(2):47–50.

[39] Chou CT, Gaur U, Miller B. Compos Sci Technol 1993;48:307.

[40] Yuan LY, Chen CS, Shyu SS, Lai JY. Compos Sci Technol 1992;45:1.

[41] Gaur U, Chou CT, Miller B. Composites 1994;25(7):609.

[42] Gaur U, Miller B. Polym Compos 1990;11(4):217.

[43] Biro DA, Pleizier G, Deslandes Y. Compos Sci Technol 1993;46:293.

[44] Latour RA, Black J, Miller B. J Compos Mater 1992;26(2):000.

[45] Gray RJ. J Mater Sci 1984;19:861.

[46] Wu HF, Claypool CM. J Mater Sci Lett 1991;10:260.

[47] Wu HF, Claypool CM. J Mater Sci Lett 1991;10:1072.

[48] Day JR, Marquez M. In: Verpoest I, Jones F, editors. Interfacial Phenomena in Composite Materials 91, Leuven, Belgique, 17–19 September 1991. London: Butterworth Heinemann, 1991. p. 73–6.

[49] Piggott MR. Compos Sci Technol 1987;30:295.

[50] Greszczuk LB. Interfaces in composites. ASTM STP. 452 42, 1969.

[51] Cox HL. Brit J Appl Phys 1952;3:72.

[52] Scheer RJ, Nairn JA. J Adhes 1995;53:45.

[53] Lawrence P, Int J. Adhes Adhes 1972;7:1.

[54] Takaku A, Arridge RGC. J Phys, Appl Phys 1973;6:2038.

[55] Hsueh CH. J Mater Sci Lett 1988;7:497.

[56] Hsueh CH. Mater Sci Engng 1990;A123:1.

[57] Hsueh CH. Mater Sci Engng 1990;A125:67.

[58] Yue CY, Cheung WL. J Mater Sci 1992;27:3173.

[59] Yue CY, Cheung WL. J Mater Sci 1992;27:3181.

[60] Outwater JO, Murphy MC. 24th Annual Technical Conference on Reinforced Plastic Division. Society of the Plastic Industries Inc., 11-C, 1969.

[61] Bowling J, Groves GW. J Mater Sci 1979;14:431.

[62] Wells JK, Beaumont PWR. J Mater Sci 1985;20:1275.

[63] Stang H, Shah SP. J Mater Sci 1986;21:953.

[64] Gao YC, Mai YW, Cotterel B. J Appl Math Phys (ZAMP) 1988;39:550.

[65] Penn LS, Lee SM. J Compos Technol Res 1989;11(1):23.

[66] Kim JK, Baillie C, Mai YW. J Mater Sci 1992;27:3143.

[67] Zhou LM, Kim JK, Mai YW. J Mater Sci 1992;27:3155.

[68] Herrera-Franco PJ, Drzal LT. Composites 1992;23:2.

[69] Venkatakrishnaiah S, Dharani LR. Eur J Mech A/Solids 1994;13(3):311.

[70] Marotzke C, Hampe A. Proceedings of ICCM-10, Whistler, Canada, VI-517, 1995.

[71] Hodzik A, Kalyanasundaram S, Lowe A, Stachurski Z. Compos Int 1999;6(4):375.

[72] DiFrancia C, Ward TC, Claus RO. Composites 1996;27A:597.

[73] Zhandarov S, Pisanova E, Lauke B. Compos Int 1998;5(5):387.

[74] Pawlak A, Zinck P, Galeski A, Gerard J. Eurofillers'99, September 6–9 1999.

[75] Williams JG. Fracture mechanics of polymers. Chichester: Ellis Horwood Limited, 1984.